JOURNAL OF CATALYSIS 97, 25–35 (1986)

The Effects of Water Coadsorption on the Adsorption of Oxygen over Metal Oxides

I. Temperature-Programmed Desorption Study of Co_3O_4

YUSAKU TAKITA,[1] TETSURO TASHIRO, YUMIE SAITO, AND FUMIAKI HORI

Department of Environmental Chemistry and Engineering, Faculty of Engineering, Oita University, Oita 870-11, Japan

Received June 15, 1984; revised July 8, 1985

Adsorption of oxygen and water and the effects of coadsorption of water on oxygen adsorption over Co_3O_4 were studied by means of temperature-programmed desorption (TPD). There were at least three kinds of adsorbed oxygen on the Co_3O_4 samples calcined at 823–973 K, which desorbed at 300–400, 450–600, and >600 K (denoted α, β, and γ oxygen, respectively). γ Oxygen inhibited the adsorption of α and β oxygen in the same degree. N_2O reacted with evacuated surface to evolve almost equimolar N_2 at room temperature. TPD chromatograms of oxygen from the sample with oxygen adsorbate derived from N_2O decomposition well agreed with those from the sample with a corresponding amount of oxygen adsorbate formed from oxygen preadsorption in regard to peak shape and peak maximum temperature. The TPD experiments using $^{18}O_2$ revealed that oxygen exchange between oxygen adsorbates and oxide ions of the Co_3O_4 sample took place above 323 K, and the equilibration of isotopes among oxygen adsorbates was observed even below 323 K. Dissociative adsorption of oxygen appears to be compatible with the experimental results. TPD of water from Co_3O_4 preadsorbed with varied amount of water disclosed the presence of four kinds of adsorbed water which desorbed at 300–450, 450–550, 550–700, and >700 K. Preadsorption of water at 473 K brought about the slight decrease of γ oxygen and the rearrangement of α and β oxygen to ε oxygen (350–450 K) without change of the total amount of oxygen desorbed.

INTRODUCTION

In the catalytic oxidation of olefins over metal oxides, it has been known that water vapor addition into the reaction system enhances the yield of desired products (*1–5*). In the catalytic oxidation of organic substances, most reactions are accompanied by a side reaction leading to the formation of water. Therefore, even if feed gas contains no water vapor, water molecules (a by-product), may accumulate on the catalyst surface during the reaction. This will, more or less, affect the adsorption of reactants, products, and/or intermediates. The oxidation of methyl ethyl ketone (MEK or 2-butanone) over Co_3O_4 is such a case (*6, 7*). MEK was oxidized to a couple of acetaldehyde and acetic acid over the dry Co_3O_4 surface, but accumulation of water on the surface made biacetyl formation superior.

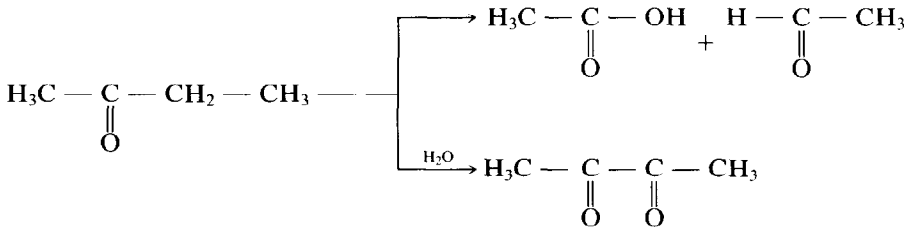

[1] To whom correspondence should be addressed.

0021-9517/86 $3.00

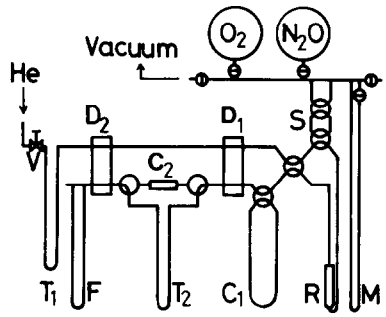

FIG. 1. Schematic diagram of TPD apparatus. C_1, SiO_2 gel column (3 mm i.d., 2 m); C_2, molecular sieves 13X column (3 mm i.d., 1 m); D_1 and D_2, thermal conductivity detector; F, flow meter; M, Hg manometer; R, TPD cell, S, sampler; T_1 and T_2, cold trap (liq. N_2); V, mass flow valve.

The water adsorbed on the metal oxide surfaces has been studied using various methods such as infrared spectroscopy (*8*), kinetics (*9*), temperature-programmed desorption (*10, 11*), SIMS-Auger (*12*), and so on. The properties of the surface hydroxyl on Al_2O_3, SiO_2, TiO_2, and ZnO, which are utilized as catalyst supports, are relatively well understood. However, little is known about the adsorption of water on metal oxides which are claimed to be effective for the oxidation of hydrocarbons and how surface hydroxyl affects other adsorbate on the metal oxides (*6, 13*).

In this series of studies, an attempt was made to investigate the interaction between adsorbed water and oxygen adsorbate on metal oxides and the effects of adsorbed water on the reactivity of oxygen adsorbate. The first report of this series, deals with the adsorption state of oxygen and water and the effect of surface hydroxyl on the TPD of oxygen over Co_3O_4.

EXPERIMENTAL

Sample Preparation

Co_3O_4 was prepared from thermal decomposition of $Co(NO_3)_2 \cdot 6H_2O$ (Wako Pure Chem. Ind., pure grade) at 573 K for 2 h in the air, then the powder formed was pressed into cylindrical form at 500 kg/cm^2 for 1 min. The granules of the sample (24–32 mesh) were calcined in the air at the desired temperature for 4 h. Unless otherwise noted, the sample calcined at 823 K was used for experiments.

Analysis of Samples

The purity of all samples was confirmed by X-ray powder diffraction. The analysis of nitrogen content was carried out by the procedure described in the literature (*14*). NO_3^- extracted from the Co_3O_4 sample calcined at 823 K was reduced to NO_2^-, which was converted to diazonium cation by reacting with sulfuric acid. It was then complexed with α-naphthyl amine and the concentration was determined by the absorption at 520 nm.

Apparatus and Method

TPD apparatus used here was basically the same as that described in the literature (*15*), and a schematic diagram of the apparatus is depicted in Fig. 1. TPD chromatograms were recorded at a constant heating rate 20 K/min under a He flow rate of 30 cm^3/min. Desorption chromatograms of water were obtained from the comparison of the chromatograms recorded with two thermal conductivity detector (D_1 and D_2) located at upper stream and at lower stream of the cold trap (T_2) kept at liquid-nitrogen temperature for the removal of water vapor.

Fresh Co_3O_4 sample (1.5 g) loaded into the TPD cell was evacuated at 793 K at $<10^{-5}$ Torr (1.33×10^{-3} N/m^2) for 1 h. Then, the sample was subjected to the standard oxygen pretreatment (SOP) composed of the exposure to oxygen at 100 Torr for 1 h and subsequent evacuation at 793 K for 1.5 h. SOP was achieved prior to each experimental run. Adsorption of water and oxygen was carried out by either of the procedures listed in Table 1.

The concentration of oxygen isotopes was determined by ULVAC MSQ150A quadrupole mass analyzer.

TABLE 1

Adsorption Procedures of Gases

Procedure	Step 1	Step 2	Step 3
I	Exposure to 100 Torr O_2 at 793 K for 0.5 h	Cooling to 278 K at a rate of 10 K/min	Evacuation at 278 K for 0.25 h
II	Exposure to 100 Torr O_2 at 473 K for 0.5 h	Cooling to 278 K at a rate of 10 K/min	Evacuation at 278 K for 0.25 h
III	Introduction of water vapor at 793 K for 0.5 h	Cooling to 278 K at a rate of 10 K/min	Evacuation at 278 K for 0.25 h
IV	Introduction of water vapor at 473 K for 0.5 h	Cooling to 278 K at a rate of 10 K/min	Evacuation at 278 K for 0.25 h
V	Introduction of water vapor at 473 K for 0.5 h	Evacuation at 473 K for 0.25 h	Proc. II

RESULTS AND DISCUSSION

TPD of Oxygen Adsorbed on Co_3O_4

The thermodesorption of adsorbate on solid surface is normally carried out under vacuum or in an inert gas stream such as He in TPD study. It is of importance whether the TPD chromatogram obtained in He stream reflects the situation under the reaction conditions since molecular oxygen is present in gas phase in the catalytic oxidation. From this point of view, TPD of oxygen was examined using He + O_2 carrier and the result is shown in Fig. 2 together with the result using He carrier. As shown in the figure, both spectra agreed excellently with each other except for the peaks at near room temperature. The discrepancy of the peaks indicates that a small amount of oxygen is adsorbed reversibly in the presence of gas-phase oxygen only at near room temperature. These oxygen peaks, however, are believed to be not important for catalytic oxidation because the IR spectrum of the Co_3O_4 wafer exposed to the mixture of oxygen and MEK at room temperature was unchanged until after 2 days and most of the catalytic oxidations are carried out at more than 400 K. It was concluded from this result that TPD in He carrier reflected the oxygen adsorption during catalytic oxidations.

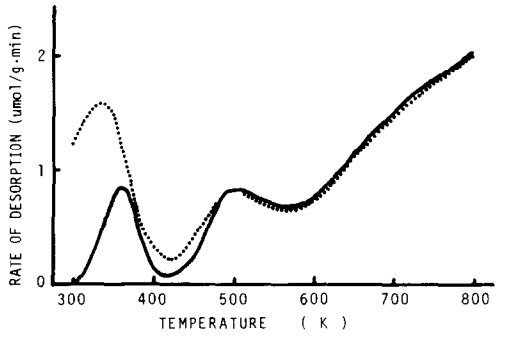

FIG. 2. TPD chromatogram of oxygen. The effect of carrier gas. (———) He carrier, (· · ·) He + O_2 (0.14 mol%) carrier. Oxygen preadsorption: Proc.I.

TPD chromatograms of oxygen from the sample preadsorbed at different temperatures are shown in Fig. 3. Preadsorption at 298 K gave the oxygen desorption with the peak at 383 K and the ascent at 600 K (curve a). The TPD chromatogram from the sample preadsorbed by Proc. II (curve b) consisted of two desorption peaks with the peak maxima at 363 and 500 K and the ascent at >700 K, which are designated here as α, β, and γ oxygen, respectively. Desorption peaks with the maxima at 360 and 500 K and a broad desorption at >600 K were obtained from the sample preadsorbed at 793–278 K (curve c). Although the peak maximum temperature (T_m) of α oxygen in curve a was slightly higher than those in curves b and c, T_m of α and β oxygen in

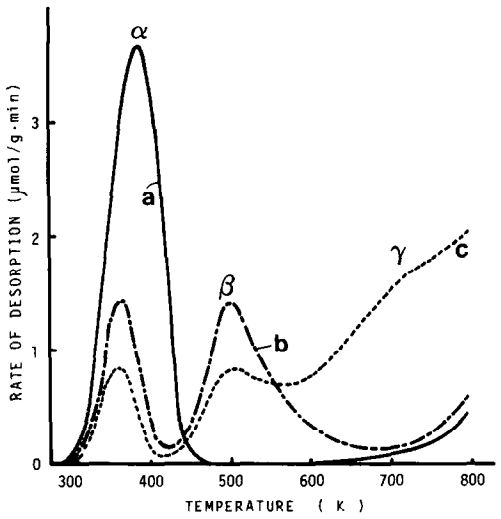

FIG. 3. TPD chromatograms of oxygen. The effect of preadsorption temperature: (a) 298 K, (b) 473–278 K (Proc.II), (c) 793–278 K (Proc.I).

curves b and c were in fair agreement with each other. These results revealed that there are at least three kinds of oxygen adsorbates on the surface of Co_3O_4.

As for the TPD of oxygen on Co_3O_4, two studies have been reported: Iwamoto *et al.* (*16*) obtained the desorption peaks with T_m at 303, 438, and 653 K from the Co_3O_4 sample exposed to oxygen at 872–273 K; Cruz *et al.* (*17*) reported three desorption peaks with T_m at 300, 550, and 778 K. Although T_m in this work does not agree with those in both studies, however, reproducibility of the chromatogram was fairly good in the present study. The nitrogen content of the sample was determined to be 0.00204 wt% which was, adequately, a low level. It was confirmed by a separate experiment using the Co_3O_4 sample prepared from cobalt carbonate that T_m of oxygen peaks were identical with those from the sample prepared from cobalt nitrate. This fact strongly suggested that no residual nitrate anions caused the discrepancy of T_m. The inconsistency with the latter work may be mainly due to the difference in heating rate because it was accomplished by the flash desorption method (5–7 K/s). The inconsistency with the former work adopting the similar experimental method to that in this study may be due to the differences of preadsorption procedure and of the source (hydroxide) of the Co_3O_4 sample.

The amount of oxygen desorbed in TPD is summarized in Table 2. Increase of the preadsorption temperature enhanced the total amount of oxygen desorbed. However, it is noted that the total amount from the sample preadsorbed at 298 K was slightly larger than that at 473–278 K. As for α oxygen, the desorbed amounts in curves b and c were considerably small compared with that in curve a, while T_m in b and c were lower than that in a by 20 K. The heterogeneity of the sites on the oxide surface cannot account for the results because T_m should be shifted to lower temperatures with increasing surface coverage. This shift was actually observed for oxygen in a later section (Fig. 7). It may, therefore, be caused by the copresence of β oxygen.

In the course of oxygen adsorption of Proc.II, the adsorption of β oxygen would be accomplished at >425 K, and the adsorption of α oxygen would succesively take place during the cooling process. Comparing curves a and b, it can be seen that the amount of α oxygen was reduced from 11.8 to 3.56 μmol/g by the copresence of β oxygen (6.20 μmol/g). In other words, adsorbed β oxygen inhibited the adsorption of α oxygen by about 1.3 mol/mol β oxygen. The above-mentioned shift of T_m along with the inhibition strongly suggests that the adsorption sites for both α and β oxygen were situated in positions which approached

TABLE 2

The Effect of Preadsorption Temperature on the Amount of Oxygen Desorbed

Oxygen adsorption	Amount of oxygen desorbed (μmol/g)				Curve in Fig. 2
	α	β	γ	Total	
298 K	11.79	0.29	1.09	13.18	a
Proc.II (473 → 278 K)	3.56	6.50	1.18	11.23	b
Proc.I (798 → 278 K)	2.06	3.82	12.99	18.88	c

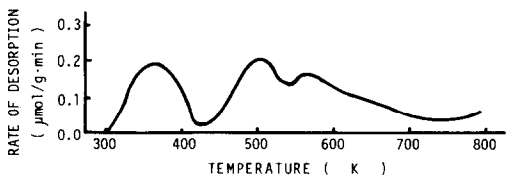

FIG. 4. TPD chromatograms of oxygen from the Co_3O_4 sample calcined at 1073 K. Oxygen preadsorption: Proc.II.

closer to each other. Similarly, the appearance of γ oxygen brought about the decrease of the amount of α and β oxygen by the same magnitude. This may also support this presumption.

The specific surface area of the sample calcined at 823 K was determined to be 29.4 m^2/g by the BET method. The sample showed the X-ray powder pattern characteristic of Co_3O_4 of spinel structure and did not appear to contain any amorphous phase. The crystal domain size was calculated to be 33.5 nm from X-ray dispersion. Assuming the spheres of 33.5 nm diameter, specific surface area was calculated to be 29.5 m^2/g using specific gravity of Co_3O_4 spinel, 6.07 g/cm^3. This value is surprisingly in good agreement with the value by BET method.

Pore size distribution of the sample was also measured by the method using adsorption isotherm of nitrogen. No prominent maximum was observed in the pore size distribution in the diameter range 1–30 nm and total volume of pores was determined to be 0.054 cm^3/g. These results indicated that the Co_3O_4 sample had relatively low porosity. Thus, the amount of oxygen desorbed was tentatively compared with surface cobalt atoms of low index planes of Co_3O_4 spinel. The number of surface cobalt atoms on (100), (110), and (111) planes of Co_3O_4 spinel are calculated to be 9.18×10^{14}, 8.66×10^{14}, and 8.44×10^{14} atoms/cm^2, respectively. The total amount of desorbed oxygen by Proc.I was calculated to be 3.87×10^{13} molecules O_2/cm^2. Supposing molecular and atomic types of surface oxygen species on cobalt atoms, this amount corresponds to ca. 4.4 and 8.7% of surface cobalt atoms. Not only surface defects such as edges and corners but also oxygen vacancies and dislocations may provide the sites for oxygen adsorption.

The Effects of Calcination Temperature

To obtain further information concerning the relation between the sites for α and β oxygen, TPD of oxygen from the samples calcined at 873, 973, and 1073 K were examined by Proc.II. The samples calcined at 873 and 973 K gave chromatograms which were exceedingly similar to curve b in Fig. 3 except for the peak height. That from the sample calcined at 1073 K is shown in Fig. 4 in which a new peak with T_m at 573 K appears.

The specific surface area of the samples and the surface concentration of α and β oxygen are shown in Fig. 5. With an increase the calcination temperature, the former declined, on the contrary, the latter increased monotonously. However, the ratio of β oxygen to α oxygen was independent of the calcination temperature (Fig. 6). This implies that two adsorption sites for β oxygen and one site for α oxygen form a group on the surface of Co_3O_4.

The Identification of α Oxygen

There are many studies on the identification and reactivity of oxygen adsorbates on

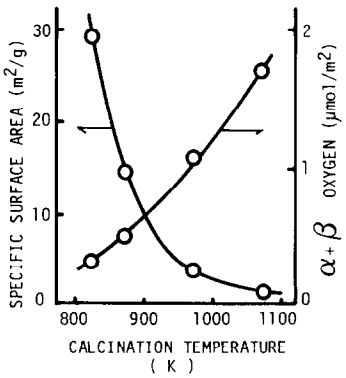

FIG. 5. The effects of calcination temperature on the specific surface area and the surface concentration of $\alpha + \beta$ oxygen.

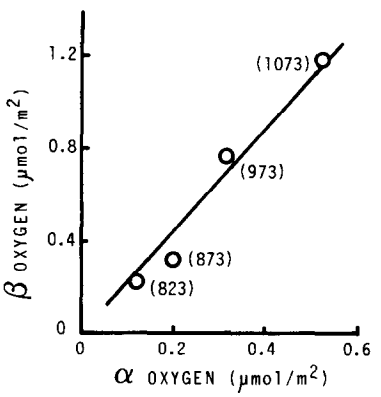

FIG. 6. The relation between the concentrations of α and β oxygen. Figures in parentheses indicate the calcination temperature.

metal oxides by means of ESR (*18*). However, most of those were performed at very low temperature and little is known about the adsorbed state of oxygen corresponding to peaks of TPD. ZnO exposed to oxygen at 283 K gave two desorption peaks with T_m at 463 and 593 K and the former peak was assigned to the desorption of O_2^- from the temperature of disappearance of ESR signal of O_2^-. The oxygen desorbed at 323–573 K on TiO_2, and the peak at 423 K on SnO_2 were similarly assigned to the desorption of O_2^- (*16*). It is recognized that the desorption temperatures of α and β oxygen are comparable to the desorption temperature of O_2^- over these oxides. So that the adsorbed oxygen species over Co_3O_4 was examined by means of ESR but no ESR signal of O^- or O_2^- was obtained though adsorption conditions were varied extensively. Cordischi *et al.* have studied the oxygen species adsorbed on CoO supported on MgO and reported that the EPR signal arose from a $Co^{3+} \cdots O_2^-$ species was observed only in the presence of oxygen in the gas phase but this species was easily destroyed by the evacuation at 298 K (*19*). This suggests the difficulty of the formation of the molecular-type oxygen adsorbate on the Co_3O_4 surface.

Therefore, two experiments were achieved to estimate the adsorption state of oxygen corresponding to the peaks of TPD.

Usually, N_2O decomposes on metal oxides to give an atomic type of oxygen species, thus the reaction between N_2O gas and the Co_3O_4 surface, and the TPD of the resultant adsorbates on the surface were studied. About 6.0–6.4 μmol of N_2O gas was introduced into He stream using the sampler (S in Fig. 1). All of the introduced gas were adsorbed by the Co_3O_4 sample in the TPD cell at 298 K and evolved N_2 gas in the effluent gas. It was analized quantitatively using the columns of silica gel and molecular sieves as depicted in Fig. 1. The sample, after the reaction with N_2O, was then submitted to TPD measurement.

The results are shown in Fig. 7 and Table 3. The amounts of reacted N_2O approximately agreed with that of effluent N_2 in each run, suggesting that there was no adsorbed molecular N_2O on the sample. TPD chromatograms of oxygen from the sample with oxygen adsorbates derived from N_2O were mainly composed of α oxygen. The amount of β and γ oxygen were very small and it seemed to be constant except for the one in run 1 in which a very small oxygen was adsorbed. On the contrary, the amount of α oxygen increased in proportion to the amount of N_2O reacted. The experiments using molecular oxygen were achieved on

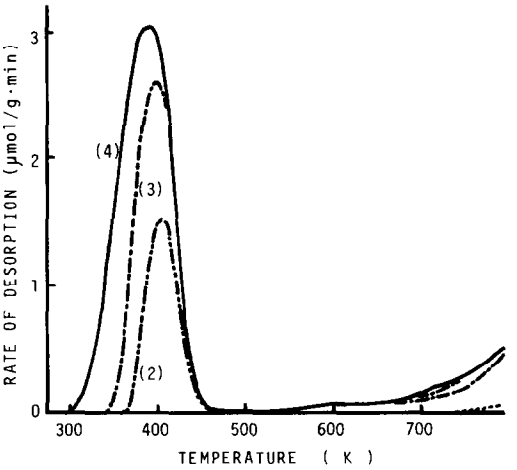

FIG. 7. TPD chromatograms of oxygen adsorbate derived from N_2O decomposition. Figures in parentheses indicate run No. in Table 3.

TABLE 3

Reaction of N_2O with Co_3O_4 Surface and TPD of Oxygen from Co_3O_4 with Adsorbate Derived from N_2O

Run No.	Amount of gas (μmol/g)				Amount of oxygen (μmol/g)			
	N_2O		N_2 flowed out	O_2 adsorbed	Desorbed			Adsorbed irreversibly
	Introduced	Reacted			α	β	γ	
1	4.13	3.98	3.97	1.99	0.007		0.12	1.86
2	16.56	15.11	14.85	7.43	3.49	0.45	1.51	1.98
3	24.92	23.01	22.13	11.07	7.27	0.35	1.09	2.35
4	36.67	32.60	30.65	15.33	11.35	0.44	1.63	1.91

the identical Co_3O_4 sample under the same experimental conditions as in the case of N_2O. The results completely coincided with that of N_2O in respect to the peak shape, T_m, and the amount of desorption. The surface oxygen atoms formed from N_2O decomposition in run 4 were calculated to be about 7.1% of surface cobalt atoms. This value is appreciably small so that all of the atomic adsorbates derived from N_2O might not be transformed to molecular ones. From these results, it appears that α oxygen is composed of an atomic adsorbate.

The adsorption state of α oxygen was studied further by the use of ^{18}O tracer. At first, oxygen atom exchange between the oxygen adsorbate and oxide ions in the bulk Co_3O_4 was examined. The sample was exposed to $^{18}O_2$ at 298 K for 30 min for preadsorption, after the evacuation at the same temperature the sample was subjected to the ordinary TPD measurement and the desorbing gas was analized continuously by mass spectrometer. The results are shown in Fig. 8a. The desorbed oxygen abounded in $^{18}O_2$ at lower temperatures, however, as the temperature was increased, the formation of $^{18}O^{16}O$ was encouraged and $^{16}O_2$ appeared above 373 K. The total amount of oxygen desorbed from the sample was determined to be 17.0 μmol which was extremely smaller than ca. 430 μg-atom of the surface oxide ions. The concentration of ^{16}O in the desorbed gas was calculated to be ca. 18.4 at.% which suggested that only the oxide ions located in surface and subsurface layers could participate in the exchange under these experimental conditions.

Another experiment was carried out using the fresh Co_3O_4 sample and equimolar mixture of $^{16}O_2$ and $^{18}O_2$ under the same experimental conditions as those described above. The results are shown in Fig. 8b. Desorbed oxygen attained equilibrium in concentration even below 325 K and the concentration of $^{18}O^{16}O$ and $^{18}O_2$ decreased with increasing temperature due to the contribution of exchange with bulk oxide.

If the two processes, associative oxygen adsorption and the rapid exchange among the adsorbates, take place together, the concentration curves of oxygen isotopes will be similar to those in the case of dissociative oxygen adsorption. However, it is evident that the results of the tracer studies are at least not inconsistent with the formation of atomic adsorbate.

Taking into account the results of N_2O experiment and ESR studies, α oxygen is believed to be composed of an atomic-type oxygen species on the Co_3O_4 surface, as similarly reported on Cr_2O_3 (*20–22*).

The Activation Energy of Desorption of α Oxygen

The activation energy of desorption (E_d) for α oxygen was determined. For second-order desorption from homogeneous sur-

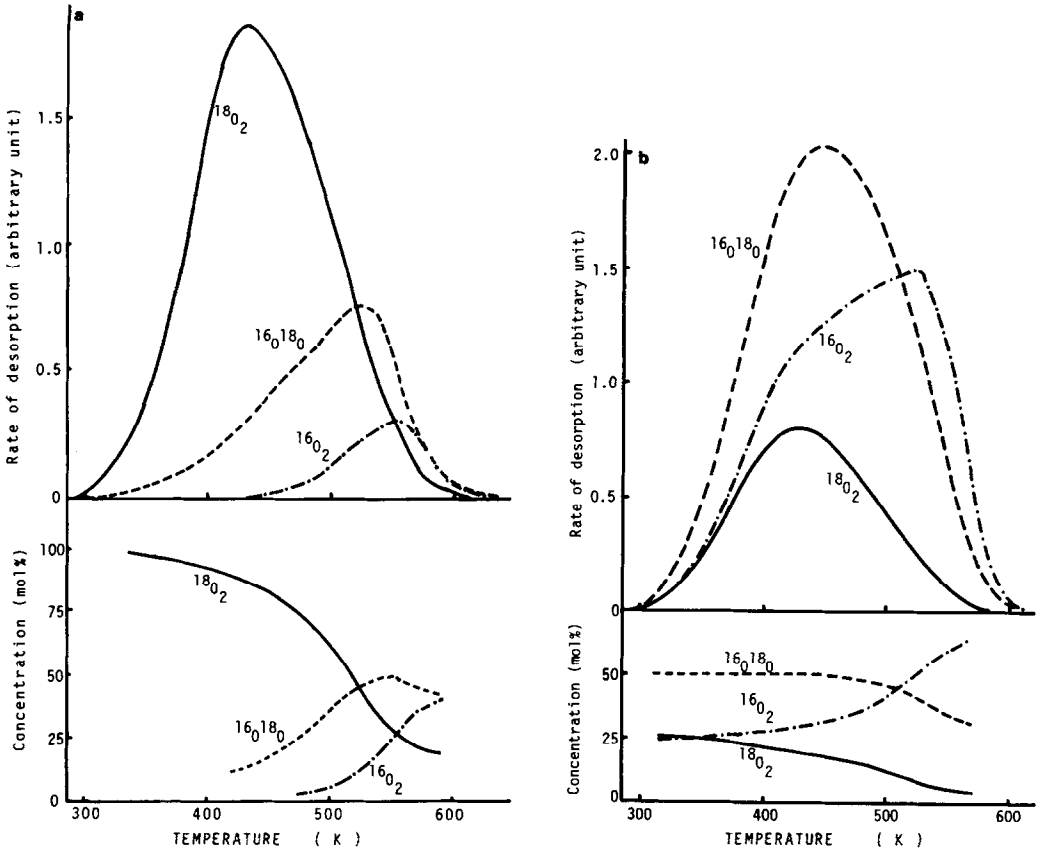

FIG. 8. (a) Oxygen exchange between adsorbate and bulk oxide. (b) Oxygen exchange among adsorbates.

face, T_m is correlated with E_d and heating rate b by the equation

$$2 \ln T_m - \ln b = \frac{E_d}{RT_m} + \ln \frac{E_d}{2AR\theta_m},$$

where R, A, and θ_m are gas constant, preexponential factor, and fractional surface coverage at T_m, respectively (*14*). Thus, E_d can be obtained from the plot of $2 \ln T_m - \ln b$ vs $1/T_m$ when θ_m is constant. Such an analysis was applied to α oxygen. θ_m showed constant value (0.592–0.600) in the experiments with b = 5, 10, and 20 K/min, therefore, E_d = 66.9 kJ/mol was obtained from the slope of the above plot. This value is reasonable when compared with 113.8 kJ/mol for the peak at 653 K (*16*).

TPD of Water

The desorption of water was examined at 298 K. The results are shown in Fig. 9. When a small amount of water was preadsorbed (curve a), desorption of water was observed only above 500 K and the chromatogram was composed of a peak with T_m at 650 K and ascent above 700 K. In addition to these, a new peak with T_m at around 510 K appeared in the chromatogram as the amount of water for preadsorption was increased (curve b). When a large amount of water was preadsorbed, a large desorption peak with T_m at 425 K (curve c) appeared with the shoulder peaks which were identical with those in curves a and b. The relative coverage of surface cobalt atoms by

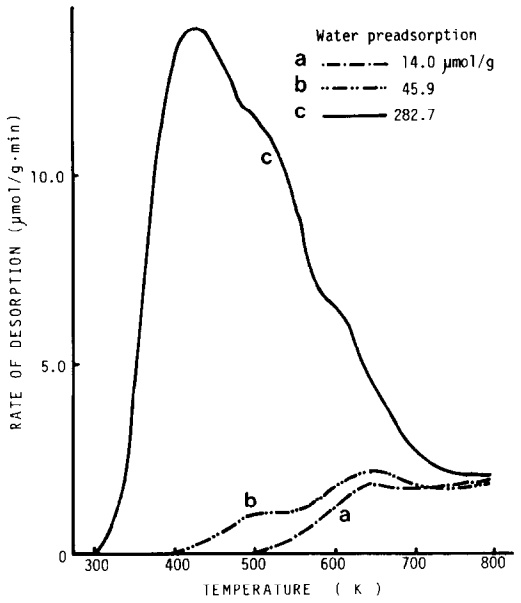

FIG. 9. TPD chromatograms of water. Preadsorption temperature: 298 K.

water was determined to be about 75% for curve c. These results revealed that there were at least four kinds of water adsorption on Co_3O_4.

It has been known that water can be chemisorbed onto metal oxide surfaces to give surface hydroxyl. Desorption temperature of chemisorbed water was characteristic of each metal oxide. Morimoto and Naono investigated the adsorption isotherm of water vapor by means of the volumetric method and showed that the surface hydroxyl began to desorb at around 383 and 473 K from the surfaces of TiO_2 and ZnO, respectively (*23*). Although this temperature is still not known for Co_3O_4, it seems reasonable to conclude that the peaks with T_m above 500 K originated from surface hydroxyls.

The Effects of Water Coadsorption on the Adsorption of Oxygen

In order to examine the effect of chemisorbed water on the adsorption of oxygen, the desired amount of water was chemisorbed on the Co_3O_4 sample at 473 K. After the evacuation at the same temperature, the sample was subjected to the oxygen adsorption process (Proc.V). The results are depicted in Figs. 10 and 11. A small amount

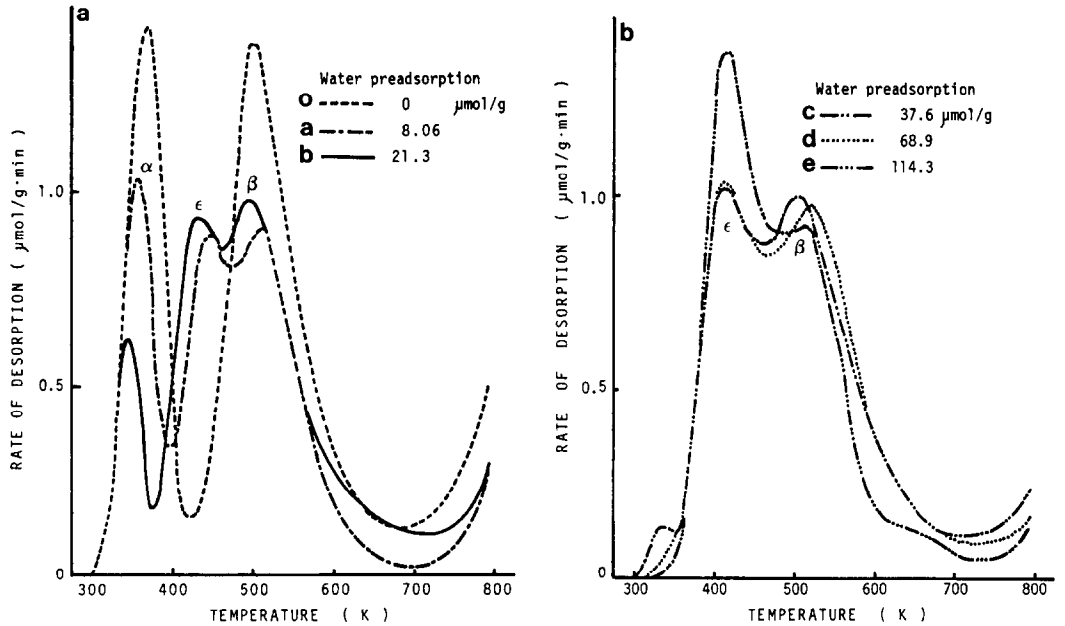

FIG. 10. TPD chromatograms of oxygen. The effects of water coadsorption. Preadsorption: Proc. V.

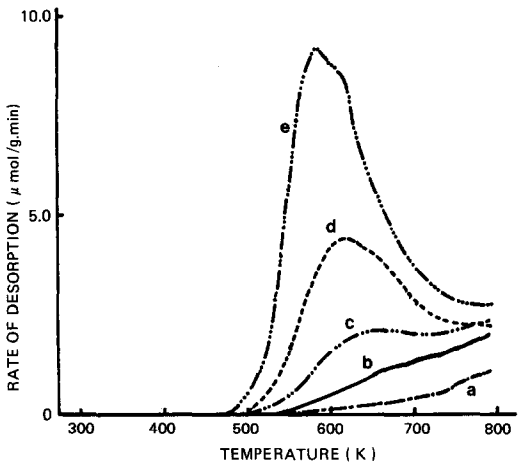

FIG. 11. TPD chromatogram of water. Letters correspond to those in Fig. 10.

of water preadsorption brought about a drastic change in the desorption chromatogram of oxygen. The peak of α oxygen became smaller with the shift of T_m to 356 K, and that of β oxygen was also reduced but a new desorption peak appeared between α and β oxygen peaks which was referred to as ε oxygen. By increasing the water preadsorption (curves b–d), the peak of α oxygen declined gradually and finally disappeared. On the contrary, ε oxygen grew in size to almost that of the original α oxygen. β Oxygen, however, seemed basically unchanged in the curves a–e.

As for the desorption of water, when the amount of adsorption was small, the chromatograms were composed of the ascent at above 550 K (curves a and b in Fig. 11). By the increase of water preadsorption, the peak at around 600 K became distinct (curve c), and it increased with the shift of T_m to lower temperatures (curves d and e). It should be noted that all of the introduced water was chemisorbed onto Co_3O_4 in this experiment.

Because of the difficulty in determination of the amount of α, β, and ε oxygen individually, the amounts of oxygen desorbed at the temperatures from 300 to 673 K (the sum of α, ε, and β oxygen) and from 673 to 793 K (γ oxygen) were determined tentatively and were plotted against the amount of preadsorbed water in Fig. 12. Chemisorbed water inhibited the adsorption of γ oxygen even at a very low relative coverage of surface cobalt atoms. On the other hand, the amount of ($\alpha + \varepsilon + \beta$) oxygen remained unaltered at least until 30% of surface cobalt atoms was covered with chemisorbed water. This means that chemisorbed water did not inhibit the adsorption of α and β oxygen. The rearrangement of β oxygen was observed only at very small amounts of water for preadsorption, suggesting that the surface hydroxyls desorbed at above 700 K interacted with β oxygen.

The amount of water required to rearrange all of the α oxygen to ε oxygen was determined to be 8.7×10^{13} molecules/cm^2, which corresponds to 9.8% of the relative coverage of surface cobalt atoms. At the same time, 14.4% of surface cobalt atoms was covered by oxygen and hydroxyl group, so that not only edges and corners but also oxygen vacancies and dislocations provided the adsorption sites. Perhaps, Co ions with high coordinative unsaturation such as Co ions on (100) plane of spinel structure may provide adsorption sites for α and β oxygen.

The authors assume that the partially negatively charged atomic oxygen species on the surface Co ions interacted with sur-

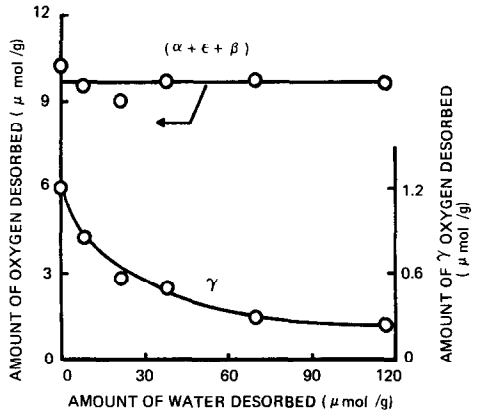

FIG. 12. The effects of the amount of coadsorbed water on the amount of oxygen desorbed.

face hydroxyl on a Co ion located at nearest neighbor through a hydrogen bond. A tracer study may give further information in this respect.

MEK is oxidized to biacetyl with a measurable rate at 400 K over Co_3O_4. Therefore, no α oxygen can exist on a dry surface under the catalytic reaction conditions, on the contrary, ε oxygen will be present on a wet surface. Resultant increase in the concentration of adsorbed oxygen on the catalyst surface may account for the enhancement of catalytic activity in the system containing water vapor. Studies on whether ε oxygen participates directly in the biacetyl formation reaction, and the effect of water (surface hydroxyl) on the adsorption of MEK are now in progress.

ACKNOWLEDGMENTS

The authors are grateful to Oita Research Center of Showa Denko K.K. for analysis by X-ray powder diffraction. Thanks are due to Mr. T. Yoko-o for the measurement of pore distribution.

REFERENCES

1. Bond, G. C., "Heterogeneous Catalysis." Oxford Univ. Press (Clarendon), London/New York, 1974.
2. Garnish, A. M., Shafranskii, L. M., and Skvortsov, N. P., *Kinet. Katal.* **3,** 257 (1962).
3. Popova, E. N., and Gorokhovatskii, Ya. B., *Dokl. Acad. Nauk. SSSR* **145,** 570 (1962).
4. Mann, R. S., and Rouleau, D., *J. Chem. Soc.*, 5471 (1964).
5. Takita, Y., Nita, K., Maehara, T., Yamazoe, N., and Seiyama, T., *J. Catal.* **50,** 364 (1977).
6. Takita, Y., Iwanaga, K., Yamazoe, N., and Seiyama, T., *Oxid. Commun.* **1,** 135 (1980).
7. Yamazoe, N., Noguchi, M., and Seiyama, T., *Nippon Kagaku Kaishi,* 470 (1980).
8. Peri, J. B., *J. Phys. Chem.* **69,** 211 (1965).
9. Boehm, H. B., "Advances in Catalysis," Vol. 16, p. 179. Academic Press, New York, 1966.
10. Morimoto, T., and Naono, H., *Bull. Chem. Soc. Jpn.* **46,** 2000 (1965).
11. Egashira, M., Kawasumi, S., Kagawa, S., and Seiyama, T., *Bull. Chem. Soc. Jpn.* **51,** 3144 (1978).
12. Paue, E. De., and Marien, J., *J. Phys. Chem.* **85,** 3550 (1981).
13. Egashira, M., Nakashima, M., and Kawasumi, S., *J. Chem. Soc. Chem. Commun.*, 1047 (1981).
14. Streuli, C. A., and Averell, P. R., "The Analytical Chemistry of Nitrogen and Its Compounds." Wiley–Interscience, New York, 1970.
15. Amenomiya, Y., and Cvetanovic, R. J., *J. Phys. Chem.* **67,** 144, 2046, 2705 (1963).
16. Iwamoto, M., Yoda, Y., Egashira, M., and Seiyama, T., *J. Phys. Chem.* **80,** 1989 (1976).
17. Cruz, L. G., Joly, J. P., and Germain, J. E., *J. Chim. Phys. Chim. Biol.* **75,** 324 (1978).
18. Stephenson, L. M., *Acc. Chem. Rev.* **13,** 419 (1980); Lunsford, J. H., "Advances in Catalysis," Vol. 22, p. 265. Academic Press, New York, 1972; *Catal. Rev. Sci. Eng.* **8,** 135 (1973).
19. Cordischi, D., Indovina, V., Occhiuzzi, M., and Arieti, A., *J. Chem. Soc. Faraday Trans. I* **75,** 533 (1979).
20. Zecchina, A., Colluccia, S., Cerrutti, L., and Borello, E., *J. Phys. Chem.* **75,** 2783 (1971).
21. Zecchina, A., Colluccia, S., Guglielminotti, E., and Ghiotti, G., *J. Phys. Chem.* **75,** 2774 (1971).
22. Zecchina, A., Guglielminotti, E., Cerrutti, L., and Colluccia, S., *J. Phys. Chem.* **76,** 571 (1972).
23. Morimoto, T., and Naono, H., *Bull. Chem. Soc. Jpn.* **41,** 1533 (1968).